

1 **Interpreting the Dependence of Cloud-Radiative**
2 **Adjustment on Forcing Agent**

3 **Pietro Salvi¹, Paulo Ceppi¹, Jonathan M. Gregory^{2,3}**

4 ¹Department of Physics & Grantham Institute, Imperial College London, London, UK

5 ²National Centre for Atmospheric Science, University of Reading, Reading, UK

6 ³Met Office Hadley Centre, Exeter, UK

7 **Key Points:**

- 8 • Cloud adjustment depends on the “characteristic altitude” of the atmospheric heat-
9 ing profile
10 • Boundary-layer (free-tropospheric) heating causes positive (negative) cloud ad-
11 justment
12 • Low clouds dominate the cloud adjustment dependence on forcing altitude

Corresponding author: Pietro Salvi, pietro.salvi14@imperial.ac.uk

Abstract

Effective radiative forcing includes a contribution by rapid adjustments, i.e. changes in temperature, water vapour and clouds that modify the energy budget. Cloud adjustments in particular have been shown to depend strongly on forcing agent. We perform idealised atmospheric heating experiments to demonstrate a relationship between cloud adjustment and the vertical profile of imposed radiative heating: boundary-layer heating causes a positive cloud adjustment, while free-tropospheric heating yields a negative adjustment. This dependence is dominated by the shortwave effect of changes in low clouds. Much of the variation in cloud adjustment among realistic forcing agents such as CO₂, CH₄, solar forcing, and black carbon is explained by the “characteristic altitude” of the heating profile, through its effect on tropospheric stability.

Plain Language Summary

Changes in factors such as greenhouse gas concentrations or solar irradiance affect the balance of energy coming into vs. leaving the earth’s atmosphere, a phenomenon known as radiative forcing. This forcing can be modified by rapid atmospheric “adjustments” that occur in temperature, humidity, and cloud cover. The cloud component in particular of these rapid adjustments strongly depends on the forcing agent, for reasons that have been unclear. We find that the vertical structure of atmospheric heating explains much of the forcing agent dependence of the cloud adjustments: bottom-heavier heating causes a more positive cloud adjustment. By understanding what happens when only a small portion of the atmosphere is heated, we show that it is possible to explain cloud adjustments to more complex forcings. We anticipate that our results will provide a physical basis to understand the causes of model-to-model differences in cloud adjustments.

1 Introduction

Radiative forcing quantifies the perturbation to the Earth’s energy budget associated with a particular climatic factor, such as greenhouse gases, aerosols or solar irradiance. Forcing was originally defined as the instantaneous perturbation to the Earth’s radiative budget due to the forcing agent. Later, the concept was refined to include the effect on the tropospheric heat budget of stratospheric adjustment due to radiative changes, which are particularly important for carbon dioxide (K. Shine et al., 1995). More recently, “effective radiative forcing” (ERF) has become the usual metric (Myhre et al., 2014), which additionally accounts for relatively short-timescale tropospheric adjustments in temperature, moisture and clouds that are direct responses to the forcing, rather than being mediated by surface warming (Andrews & Forster, 2008; Gregory & Webb, 2008; Sherwood et al., 2015). This approach is justified by the fact that ERF is a better predictor of the surface temperature response than instantaneous radiative forcing (IRF) (Richardson et al., 2019) or stratosphere-adjusted forcing (K. P. Shine et al., 2003).

The rapid adjustments to radiative forcing have been found to make a substantial contribution to model uncertainty in ERF for a variety of forcing agents including anthropogenic greenhouse gases, aerosols and solar irradiance (Chung & Soden, 2015; Smith et al., 2018, 2020). Cloud adjustments account for a large part of these differences (Andrews et al., 2012; Colman & McAvaney, 2011; Smith et al., 2018; Zelinka et al., 2013), consistent with clouds being an important source of uncertainty in the response to forcing among climate models (Ceppi et al., 2017), especially in the case of aerosols. Aerosol–*radiation* interactions lead to cloud adjustments (known as semi-direct effects) by modifying local atmospheric conditions. Aerosol–*cloud* interactions lead to further cloud adjustments via microphysical changes (known as indirect effects; Bellouin et al., 2020). Only the cloud adjustments due to semi-direct effects will be considered in this paper.

Several past papers have investigated the mechanisms of cloud adjustments in response to CO₂ forcing (e.g., Dinh & Fueglistaler, 2017; Kamae & Watanabe, 2012, 2013; Kamae et al., 2015, 2019; Zelinka et al., 2013) and to absorbing aerosols such as black carbon (BC) (Ban-Weiss et al., 2012; Bellouin et al., 2020; Koch & Del Genio, 2010; Samset & Myhre, 2015; Stjern et al., 2020) or dust (Amiri-Farahani et al., 2017), but there is a lack of process studies involving other forcing agents. Smith et al. (2018) demonstrated a striking forcing agent dependence of cloud adjustments across Coupled Model Intercomparison Project phase 5 (CMIP5) models, with consistently positive adjustments to CO₂ and negative adjustments to solar and BC forcing. However, there is currently limited understanding of how different cloud adjustments arise in response to various instantaneous forcings.

In this study we address this knowledge gap by interpreting the forcing agent dependence of cloud adjustment in terms of the spatial structure of instantaneous atmospheric forcing. Specifically, we propose here that the vertical profile of atmospheric heating is a key factor for this forcing agent dependence. For absorbing aerosols, previous studies have identified a dependence of semi-direct cloud adjustments upon forcing altitude: typically positive for boundary-layer forcing, negative for free-tropospheric forcing (Amiri-Farahani et al., 2017; Ban-Weiss et al., 2012; Bellouin et al., 2020; Koch & Del Genio, 2010; Samset & Myhre, 2015; Stjern et al., 2020). Here we show that this dependence on the vertical heating profile also accounts for much of the cloud adjustment dependence on diverse forcing agents. This is demonstrated through comparison of idealised and realistic forcing experiments with a CMIP5-class climate model.

2 Data and Methods

The simulations used for this paper were run with the CAM4 model (Neale et al., 2010) in an atmosphere-only configuration with prescribed sea surface temperatures (SSTs) and sea ice concentrations. A $1.9^\circ \times 2.5^\circ$ latitude/longitude grid was used with 26 vertical levels. Simulations were run for 20 years with the climatology calculated as the average of monthly-mean data output from the model for all but the first simulated year, during which the atmosphere was adjusting to reach a steady state in the presence of the forcing. The vertical profiles shown in this paper were linearly interpolated from the model's 26 hybrid sigma–pressure levels to a finer 100-level pressure grid, with evenly spaced levels between 0 and 1000 hPa.

Instantaneous and effective radiative forcings were calculated for four forcing agents, listed in Table S1. These are among the same forcing agents as in the Precipitation Driver Response Model Intercomparison Project (PDRMIP) set of experiments (Myhre et al., 2017), although not all with the same concentrations. IRF was calculated using the Parallel Offline Radiative Transfer (PORT) tool for CAM4 (Conley et al., 2013). To obtain ERF, the difference in mean climate was taken between perturbed and control CAM4 experiments with SSTs and sea ice fixed to the control state (Hansen et al., 1997). Note that the CO₂ concentration was doubled only in the radiation scheme in the $2 \times \text{CO}_2$ experiment, so the model did not simulate a plant physiological response to CO₂, which has been found to cause significant cloud-radiative adjustments (Doutriaux-Boucher et al., 2009). Furthermore, CAM4 does not simulate aerosol–cloud interactions for black carbon, whose atmospheric concentrations are prescribed.

In addition to the realistic forcing cases (Table S1), experiments were also performed with idealised, horizontally homogeneous forcings (Table S2), prescribed as an extra heating rate in CAM4's radiation scheme. This includes uniform 4 W m^{-2} atmospheric (atm_4) and surface (sfc_4) forcing, as well as vertically-localised forcings at specific atmospheric levels ϕ (vloc_ ϕ hPa; Fig. S1). The applied heating rate anomalies for the vloc_ ϕ hPa forc-

110 ing experiments were defined as follows:

$$\begin{aligned} \Delta Q(p) &= A \cos^2 \left(\frac{(p-\phi)\pi}{2a} \right) && \text{for } (\phi - a) \leq p \leq (\phi + a) \\ \Delta Q(p) &= 0 && \text{otherwise} \end{aligned} \quad (1)$$

111 for pressure p and heating centred at ϕ , where $A = \pm 0.135 \text{ K day}^{-1}$, $a = 125 \text{ hPa}$,
 112 and ΔQ is the instantaneous atmospheric heating anomaly from the control. This pro-
 113 vides a vertically-integrated forcing of 2 W m^{-2} , except for the topmost and lowermost
 114 vertically-localised experiments which are truncated at the pressure limits (Fig. S1) and
 115 thus provide around half the vertically-integrated forcing. The whole atmosphere was
 116 covered by nine of these bounded \cos^2 heating profiles centred on multiples of 125 hPa
 117 between 0 and 1000 hPa (inclusive). The \cos^2 shape combined with the $2a$ heating pro-
 118 file widths mean that the sum of these profiles is uniform in pressure. The width a was
 119 chosen such that the forcings are sufficiently localised in the vertical, while still being
 120 adequately resolved by CAM4’s vertical grid. To test the linearity of the responses, both
 121 positive and negative vertically localised forcings were applied.

122 Rather than calculating cloud adjustments as differences in cloud-radiative effect
 123 (CRE), we use cloud kernels from Zelinka et al. (2012) (see Fig. S2). Unlike CRE dif-
 124 ferences, which are affected by non-cloud adjustments (in temperature, water vapour or
 125 surface albedo), the kernels quantify the radiative impact of cloud adjustment in isola-
 126 tion. A further benefit to using cloud kernels is that the radiative adjustments can be
 127 broken down by cloud top pressure (CTP) into contributions from high (CTP < 440 hPa),
 128 mid (440 < CTP < 680 hPa), and low (CTP > 680 hPa) clouds. To use the cloud ker-
 129 nels, the International Satellite Cloud Climatology Project (ISCCP) satellite simulator
 130 (Swales et al., 2018) was enabled in CAM4 to output the required cloud fraction histograms
 131 (see Fig. S2 for an example).

132 We introduce two measures in this paper to help understand the relationship be-
 133 tween the vertical profile of atmospheric forcing, tropospheric stability, and cloud-radiative
 134 adjustment. Firstly, to characterise the vertical distribution of forcing $Q(p)$ we define
 135 a “heating-weighted pressure centroid”:

$$\frac{\int_{p=200 \text{ hPa}}^{1000 \text{ hPa}} p \cdot Q(p) dp}{\int_{p=200 \text{ hPa}}^{1000 \text{ hPa}} Q(p) dp} \quad (2)$$

136 This is understood as the “centre of mass” of the forcing, defined such that larger val-
 137 ues here denote a bottom-heavier atmospheric forcing profile. Note that the pressure cen-
 138 troid is positive for the vertically-localised heatings of either sign. In general, the pres-
 139 sure centroid is positive and readily interpreted for atmospheric forcings which are enti-
 140 rely or mostly of the same sign at all pressures, as is the case for all those we consider.

141 Secondly, for tropospheric stability we define the “bulk tropospheric stability” (BTS)
 142 as the difference between the average potential temperature (Θ) for the 200–800 hPa layer
 143 ($\Theta_{200-800}$), taken as representative of the free troposphere, and $\Theta_{800-1000}$, taken as rep-
 144 resentative of the boundary layer:

$$\text{BTS} = \Theta_{200-800} - \Theta_{800-1000}. \quad (3)$$

145 3 Vertically Localised Atmospheric Heating Experiments

146 To gain insight into the dependence of cloud adjustments on forcing altitude, we
 147 begin with the results from the vertically-localised forcing experiments. Focusing on the
 148 vertical structure, Fig. 1 shows the global-mean adjustments of temperature (T), rela-
 149 tive humidity (RH) and cloud fraction for three of the vertically-localised forcings (cho-
 150 sen as examples). A close correspondence is found between the peak of applied heating

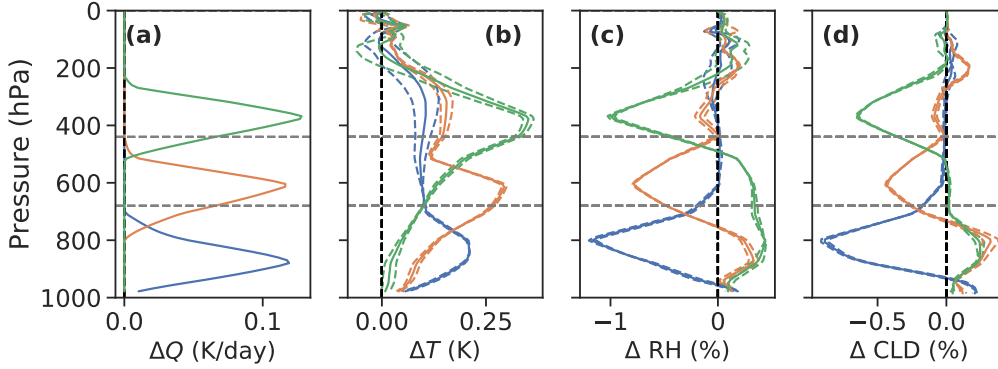


Figure 1. Profiles for (a) applied heating rates ΔQ , as well as (b) temperature, (c) relative humidity, and (d) cloud fraction (CLD) change profiles for vertically-localised heating experiments with $\phi = 875$ hPa (*blue*), $\phi = 625$ hPa (*orange*), and $\phi = 375$ hPa (*green*). Profiles shown in solid lines are the average of the positive (heating) and negative of the negative (cooling) vertically-localised forcings set at the same heights and magnitudes, with these shown separately with dashed lines. Heating profiles are interpolated from model input, rather than those defined in Eq. 1. The grey horizontal lines demarcate bounds between high, mid, and low levels according to the ISCCP simulator. Changes to temperature, relative humidity, and cloud are obtained as the difference between the equilibrium fixed SST state and a control state.

151 and the peaks of changes to T and RH, as well as cloud fraction. Furthermore, there is
 152 a striking similarity between the profiles of changes to RH and cloud fraction, as expected.

153 In addition to the expected local responses, the vertically-localised forcings also cause
 154 non-local changes via changes in stratification and their impacts on vertical heat and mois-
 155 ture fluxes. Heating at lower levels (in the boundary layer) destabilises the overlying free
 156 troposphere, leading to enhanced convection and vertical mixing and resulting in warm-
 157 ing at higher levels, but little change in RH or cloud (Fig. 1, blue curves). By contrast,
 158 free-tropospheric heating causes suppressed convection at lower levels through increased
 159 tropospheric stability (Fig. 2a, open symbols indicate greater positive ΔBTS for vertically-
 160 localised heatings at lower pressure, which means higher altitude), leading to increases
 161 to RH and cloud fraction at lower levels (Fig. 1, orange and green curves).

162 In summary, cloud fraction decreases in response to localised heating at all levels
 163 and associated drying, but low-level cloud increases in response to heating at higher lev-
 164 els. The latter is consistent with the known dependence of low clouds on tropospheric
 165 stability (Klein & Hartmann, 1993). Generally, these results are consistent with those
 166 from Samset and Myhre (2015, their Fig. 5) involving application of localised BC lay-
 167 ers at different atmospheric levels.

168 Differences between the responses to vertically-localised heating and cooling are
 169 minor (dashed lines in Fig. 1), and are mainly noticeable for the temperature response.
 170 Differences in cloud-radiative adjustments between vertically-localised positive and neg-
 171 ative heating are also minor (see discussion below).

172 There is a strong dependence of the cloud-radiative adjustments on the altitude
 173 of applied forcing and the associated stability changes. The net cloud adjustments in Fig. 2d
 174 are of substantial magnitude relative to the imposed vertically-localised forcings of 2 W
 175 m^{-2} – ranging from about -50% to $+20\%$ of the imposed forcing. This illustrates how

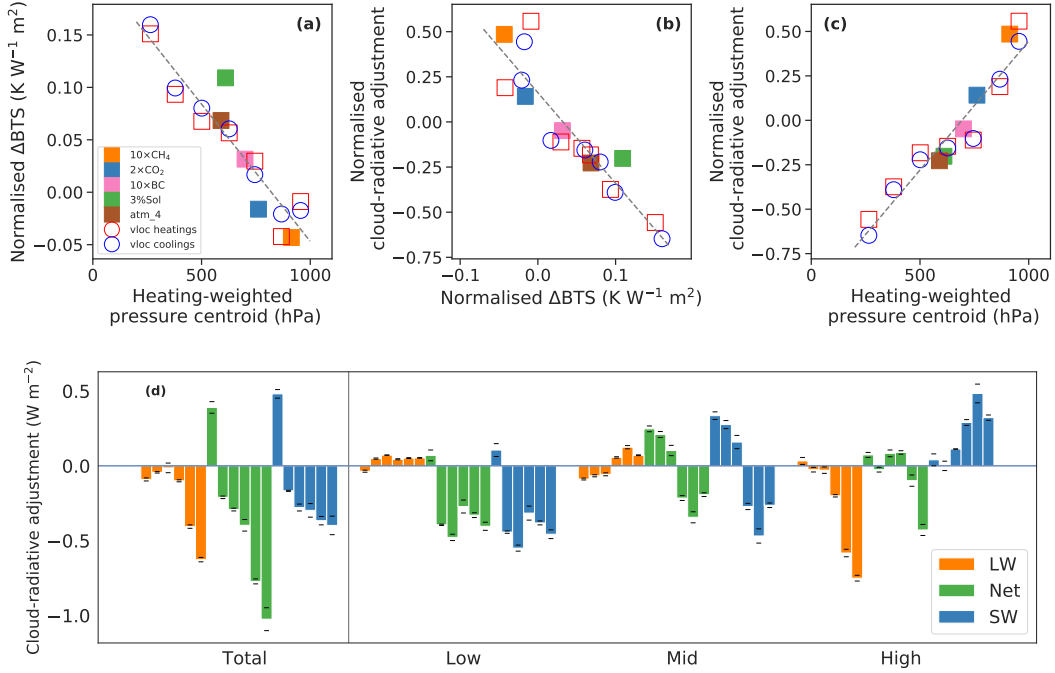


Figure 2. (a) Changes to bulk tropospheric stability (BTS, see Eq. 3), normalised by the vertically-integrated tropospheric (200–1000 hPa) forcings, versus the vertical centre of mass of tropospheric heating (Eq. 2) for each experiment performed in this study. (b) Normalised cloud-radiative adjustments against normalised BTS changes. (c) Normalised cloud-radiative adjustments versus heating centre of mass. Least-squares linear fits are shown by the dashed lines. Only experiments with significant tropospheric forcing are shown, which excludes the 0 hPa and 125 hPa forcing experiments. (d) Cloud-radiative adjustments from the six vertically-localised forcings centered between 875 and 250 hPa, in 125-hPa increments, with increasing altitude of applied heating from left to right within each coloured grouping. The lowest altitude forcing at 1000 hPa is excluded because it is truncated; furthermore, the two highest altitude forcings are excluded because they are mainly in the stratosphere, and have little impact on clouds. Individual bars represent the averages between the responses to heatings and the negative of the responses to coolings at the same altitudes and of the same magnitudes, with the thin horizontal lines around the bars representing the results from those individual experiments.

176 cloud adjustments can substantially enhance or offset the instantaneous forcing, depend-
 177 ing on the vertical distribution of heating. (Note that for the vertically localised cases
 178 the IRF equals the atmospheric heating, since there is no surface forcing, unlike in more
 179 realistic cases.) The cloud-radiative adjustment is increasingly negative with increasing
 180 height of the applied localised heating (Fig. 2c–d). This is driven by both LW and SW
 181 changes, with the latter dominating, qualitatively consistent with previous findings for
 182 BC forcing applied at different altitudes (Samset & Myhre, 2015, their Fig. 1). SW cloud
 183 adjustments flip sign from positive to negative as forcing altitude increases, while LW
 184 cloud adjustments become strongly negative (Fig. 2d). The dependence of LW cloud ad-
 185 justment on forcing altitude is consistent with the understanding that LW cloud-radiative
 186 effect increases with cloud altitude (Hartmann, 1994), due to increased temperature dif-
 187 ferences between higher clouds and the surface.

188 To interpret the dependence of SW cloud adjustment on forcing altitude, it is help-
 189 ful to consider the breakdown of the adjustments into contributions by high-, mid- and
 190 low-level clouds in Fig. 2d. The contributions are positive at the level of the heating, but
 191 negative below. This is consistent with the findings from Fig. 1: localised heating causes
 192 a cloud fraction reduction locally, but a cloud fraction increase below (particularly in the
 193 boundary layer), associated with stabilisation (Fig. 2, open symbols) and suppressed ver-
 194 tical mixing. There is an additional factor contributing to the negative SW cloud adjust-
 195 ment below the vertically-localised heating: when cloud fraction decreases at the heat-
 196 ing level, the reduced overlap reveals and hence increases SW reflection from lower-level
 197 clouds.

198 In addition to the effect of atmospheric forcing, cloud adjustments could also re-
 199 sult from surface-mediated heating. However, we find that the effect of surface forcing
 200 is very small: the net cloud-radiative adjustment for the `sfc_4` case is -0.03 W m^{-2} , with
 201 similarly small adjustment contributions across cloud altitudes and in the LW and SW.
 202 This is negligible in comparison to the adjustments for the localised atmospheric heat-
 203 ing experiments, especially per unit of forcing. This result is expected given the fixed-
 204 SST lower boundary, where surface forcing can impact the atmosphere only over land
 205 and ice regions. Note that although the rapid climate response to land warming under
 206 fixed SSTs is typically included in the ERF as part of the rapid adjustment (Forster et
 207 al., 2016; Sherwood et al., 2015), conceptually this can also be treated as a surface warming-
 208 driven radiative response (Chung & Soden, 2015; K. P. Shine et al., 2003).

209 4 Interpreting Cloud-Radiative Adjustments to Realistic Forcing Agents

210 Having established how cloud adjustments depend on the vertical profile of atmo-
 211 spheric heating in section 3, this section investigates what this information provides in
 212 understanding cloud adjustments to vertically-distributed atmospheric forcings, mainly
 213 through trying to understand adjustments to realistic forcing agents (Table S1). For each
 214 of the realistic forcings (as well as the idealised `atm_4` case) we express the vertical pro-
 215 file of global-mean IRF as a linear combination of idealised vertically-localised heatings:

$$\Delta Q_{\text{fit}}(p) = \sum_{i=1}^9 (a_i \cdot \Delta Q_i(p)), \quad (4)$$

216 where ΔQ_i and a_i are the anomalous heating rates (i.e. the IRF) and fitting coefficients
 217 respectively for each of the nine vertically-localised forcings i . The a_i coefficients were
 218 calculated so as to minimise the least-squares difference between Q_{fit} and the global-mean
 219 heating profile of a chosen case, Q_{case} (Fig. 3, left column). Best-fits are expected to be
 220 unique given that the profiles of the vertically-localised forcings are mostly non-overlapping
 221 and hence mostly orthogonal.

222 The heating profiles for the realistic forcings (and `atm_4`) are very closely approx-
 223 imated by linearly combining the nine idealised vertically-localised cases (Fig. 3, left col-

umn). The only deviations occur above the tropopause for the $2\times\text{CO}_2$ and 3%Sol cases where there is insufficient vertical resolution in the localised forcing experiments.

We then estimate the globally-averaged vertical profiles of change in temperature, relative humidity, and cloud fraction (each denoted by X) in response to vertically-distributed forcings thus:

$$\Delta X_{\text{fit}}(p) = \left(\frac{F_{\text{case,sfc}}}{4} \cdot \Delta X_{\text{sfc}_4} \right) + \sum_i (a_i \cdot \Delta X_i(p)). \quad (5)$$

The first term on the right-hand side accounts for contributions from surface forcing, using the results from a 4 W m^{-2} uniform surface forcing experiment (sfc_4, see Table S2), appropriately weighted for the surface forcing $F_{\text{case,sfc}}$ of the reference case. (Although surface forcing causes a very small adjustment per unit forcing, we found the surface contribution to be non-negligible for the 3%Sol experiment – see below.)

The linear combination of idealised vertically-localised heatings closely approximates the adjustments of temperature, RH and cloud fraction diagnosed from the model (Fig. 3). This suggests that the global-average vertical structure of these adjustments is primarily determined by the vertical profile of IRF.

The contributions to these profiles from the surface components of the forcings were found to be minor in general, consistent with our finding that the cloud adjustment to uniform surface-only forcing is very small. The notable exception to this was in the solar forcing case, where the majority of instantaneous forcing is from the surface component (4.88 W m^{-2} , compared to a 2.19 W m^{-2} atmospheric component), such that the surface component makes a non-negligible contribution to the cloud fraction change profile (Fig. S4).

Considering the global average top-of-atmosphere cloud-radiative adjustments to forcings, we find that the linear combinations of vertically-localised heating experiments generally predict the correct sign, and to a lesser extent magnitude, of the vertically-distributed forcings (Fig. 4). The largest errors are for CO_2 and CH_4 , where the positive SW adjustments are considerably underestimated. Inspection of the cloud fraction profiles in Fig. 3 suggests this may partly result from an underestimation of the lower-tropospheric cloud fraction decrease by the simple linear combination method, and potentially from differences in estimation of cloud changes near the tropopause. That the predicted net adjustments are more accurate than the individual SW and LW adjustments can be explained by compensating errors in SW and LW. Errors in this approach may also result from the linear combination of cloud-radiative adjustments being unable to account for the non-linear effects of cloud overlap.

Nevertheless, the results in Figs. 3 and 4 account for the finding of Fig. 2c (filled symbols) that the sign and magnitude of cloud-radiative adjustments are mostly explained by the vertical structure of the instantaneous atmospheric forcing, as measured by the heating-weighted pressure centroid. Positive CRE adjustments result from the “bottom-heaviest” IRFs $2\times\text{CO}_2$ and $10\times\text{CH}_4$, negative CRE adjustments from 3%Sol and atm_4, whose IRFs are fairly uniform with altitude, while 10xBC is intermediate.

Although our interpretation is based on a single climate model, we note that the cloud-radiative adjustments in Fig. 4 are reasonably representative of those simulated by a range of CMIP5 models (Fig. 4 of Smith et al., 2018). In particular, models consistently simulate positive cloud-radiative adjustments to CO_2 , and negative adjustments to solar forcing, in agreement with our results. Note that the results of Smith et al. (2018) use different magnitudes of the CH_4 and solar forcings, and include the stomatal conductance effect of $2\times\text{CO}_2$. Increases to CO_2 lead to reduced evapotranspiration and thus reduced low cloud over many highly forested areas for a positive effect on the cloud-radiative adjustment (Doutriaux-Boucher et al., 2009). We found that including this ef-

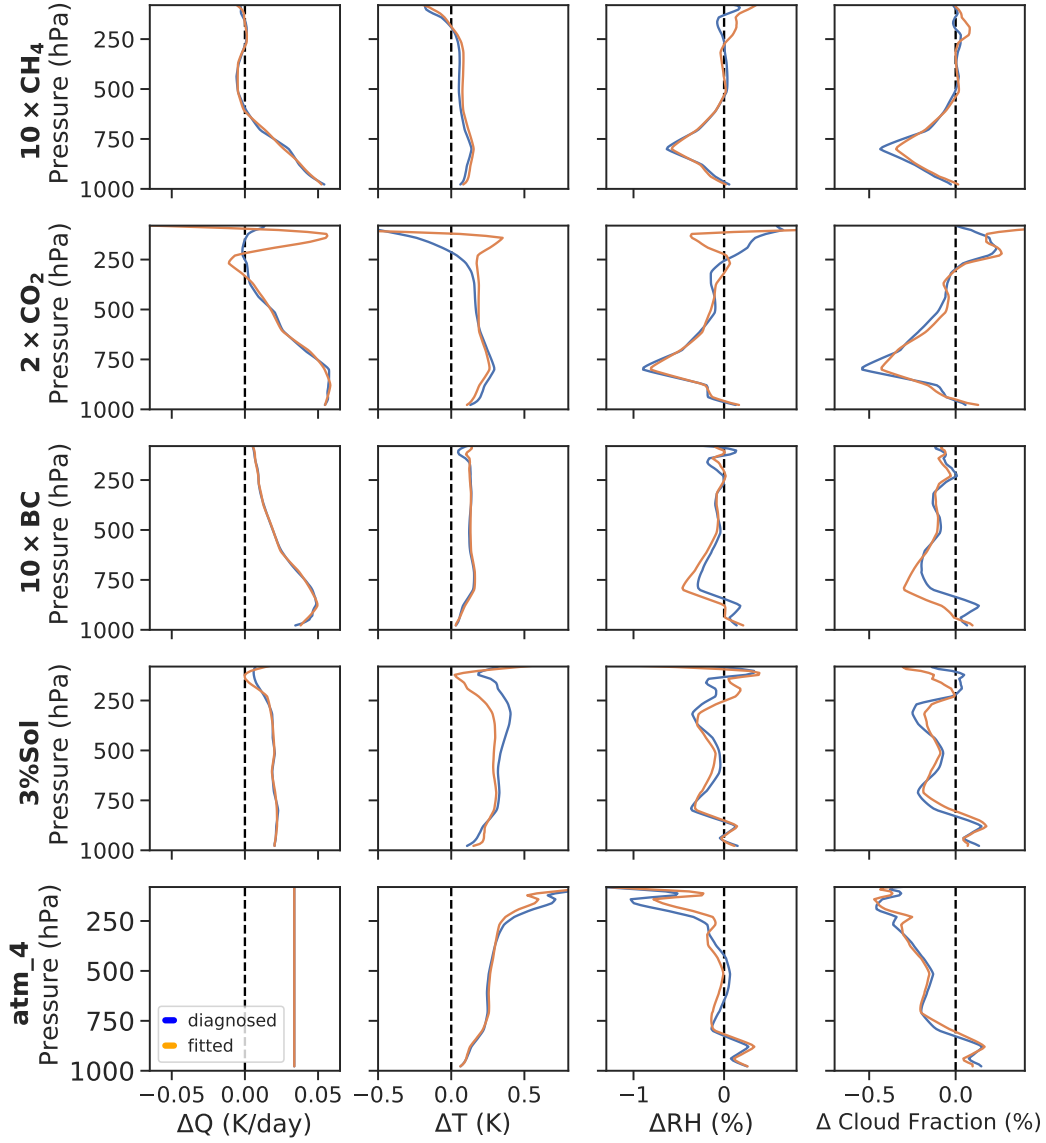


Figure 3. Global-mean vertical profiles of IRF (ΔQ) and rapid adjustments of temperature (ΔT), relative humidity (ΔRH) and cloud fraction. Shown are the results from the original cases (*blue*) and linear combinations of the results from the vertically-localised forcing experiments (*orange*) including an appropriate surface term (Eq. 5). Fitted heating rates are best fits to the original heating rates (Eq. 4), whilst the orange lines for other variables are created from the fits of heating rates (Eq. 5).

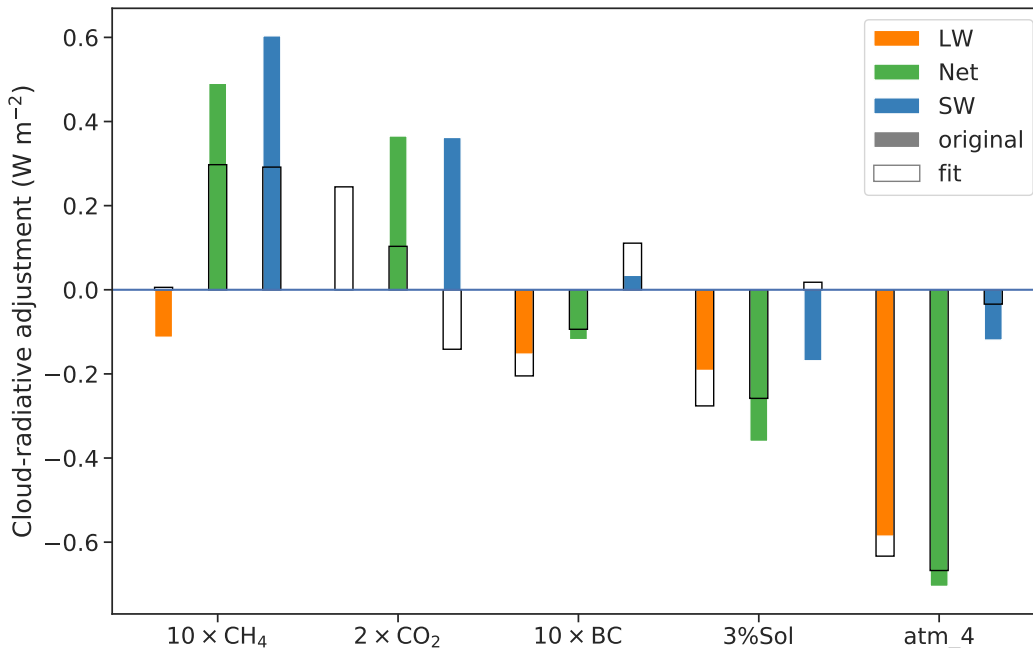


Figure 4. A comparison of the cloud-radiative adjustments predicted from linearly combining vertically-localised forcing experiments (*hatched bars*) versus the radiative adjustments calculated from the relevant experiments themselves (*solid bars*).

272 fact approximately doubles the cloud adjustment to $2\times\text{CO}_2$ forcing in CAM4 (0.76 vs
 273 0.37 W m^{-2} ; not shown).

274 5 Summary and Conclusions

275 We have demonstrated through a series of idealised experiments with vertically-
 276 localised atmospheric heating that cloud-radiative adjustments are sensitive principally
 277 to the altitude of atmospheric heating caused instantaneously by the forcing agent. At
 278 levels where there is instantaneous positive heating, the air becomes warmer and drier
 279 and the cloud fraction decreases. However, positive heating at any level above the bound-
 280 ary layer stabilises the troposphere below and suppresses vertical mixing, thus causing
 281 moistening and increased cloud fraction at lower levels. As the net result of these two
 282 effects, lower-tropospheric heating results in positive cloud-radiative adjustment (dom-
 283 inated by the SW effect of reduced low cloud fraction), while mid- and upper-tropospheric
 284 heating causes negative adjustment (due to the combined LW and SW effects of increased
 285 low cloud and reduced free-tropospheric cloud). For negative forcings, the signs of all
 286 effects are reversed and the magnitudes are similar.

287 We find that the global-mean cloud-radiative adjustments to realistic forcings can
 288 be reasonably well explained by linearly combining the idealised vertically-localised forc-
 289 ings so as to fit the vertical heating profiles caused by the various forcing agents. In par-
 290 ticular, our results suggest that positive cloud adjustment commonly found in GCMs to
 291 the greenhouse gas forcing agents CO_2 and CH_4 is explained by their relatively bottom-
 292 heavy profiles of instantaneous radiative forcing; by contrast, the negative cloud adjust-
 293 ment to solar forcing is caused by its relatively larger free-tropospheric heating. Our find-
 294 ings are consistent also with previous evidence that cloud-radiative adjustments depend

295 on the altitude of absorbing aerosols such as black carbon (Samset & Myhre, 2015; Allen
296 et al., 2019).

297 Although successful in explaining the sign and relative magnitude of adjustments
298 for different agents, our method using global-mean vertical profiles does not give quan-
299 titatively accurate estimates. This may be for instance because of neglecting the geo-
300 graphical pattern and the seasonal cycle of the instantaneous heating, perhaps especially
301 the contrast between its effects in cloudy and cloud-free air. Further investigation is needed
302 of these aspects. With such refinement, we expect that this approach will provide a use-
303 ful basis to interpret inter-model differences in cloud adjustments, to the extent that such
304 differences result from uncertainties in the distribution of instantaneous radiative forc-
305 ing.

306 **Acknowledgments**

307 PS was supported by the Department of Physics and the Grantham Institute of Impe-
308 rial College London. PC was supported by an Imperial College Research Fellowship and
309 NERC grants NE/T006250/1 and NE/T007788/1. JMG was supported by the European
310 Research Council under the European Union’s Horizon 2020 research and innovation pro-
311 gramme (grant agreement No 786427, project “Couplet”). This work used JASMIN, the
312 UK collaborative data analysis facility and the ARCHER UK National Supercomput-
313 ing Service.

314 The data that support the findings of this study are available from [https://doi](https://doi.org/10.6084/m9.figshare.14386799)
315 [.org/10.6084/m9.figshare.14386799](https://doi.org/10.6084/m9.figshare.14386799)

316 **References**

- 317 Allen, R. J., Amiri-Farahani, A., Lamarque, J.-F., Smith, C., Shindell, D., Has-
318 san, T., & Chung, C. E. (2019, December). Observationally constrained
319 aerosol–cloud semi-direct effects. *npj Climate and Atmospheric Science*,
320 *2*(1), 16. Retrieved 2020-02-04, from [http://www.nature.com/articles/](http://www.nature.com/articles/s41612-019-0073-9)
321 [s41612-019-0073-9](http://www.nature.com/articles/s41612-019-0073-9) doi: 10.1038/s41612-019-0073-9
- 322 Amiri-Farahani, A., Allen, R. J., Neubauer, D., & Lohmann, U. (2017, May). Im-
323 pact of Saharan dust on North Atlantic marine stratocumulus clouds: impor-
324 tance of the semidirect effect. *Atmospheric Chemistry and Physics*, *17*(10),
325 6305–6322. Retrieved 2021-01-25, from [https://acp.copernicus.org/](https://acp.copernicus.org/articles/17/6305/2017/)
326 [articles/17/6305/2017/](https://acp.copernicus.org/articles/17/6305/2017/) (Publisher: Copernicus GmbH) doi: [https://](https://doi.org/10.5194/acp-17-6305-2017)
327 doi.org/10.5194/acp-17-6305-2017
- 328 Andrews, T., & Forster, P. M. (2008). CO₂ forcing induces semi-direct ef-
329 fects with consequences for climate feedback interpretations. *Geophysical*
330 *Research Letters*, *35*(4). Retrieved 2021-01-12, from [https://agupubs](https://agupubs.onlinelibrary.wiley.com/doi/abs/10.1029/2007GL032273)
331 [.onlinelibrary.wiley.com/doi/abs/10.1029/2007GL032273](https://agupubs.onlinelibrary.wiley.com/doi/abs/10.1029/2007GL032273) (eprint:
332 <https://agupubs.onlinelibrary.wiley.com/doi/pdf/10.1029/2007GL032273>) doi:
333 <https://doi.org/10.1029/2007GL032273>
- 334 Andrews, T., Gregory, J. M., Forster, P. M., & Webb, M. J. (2012, July). Cloud
335 Adjustment and its Role in CO₂ Radiative Forcing and Climate Sensi-
336 tivity: A Review. *Surveys in Geophysics*, *33*(3), 619–635. Retrieved
337 2019-07-15, from <https://doi.org/10.1007/s10712-011-9152-0> doi:
338 [10.1007/s10712-011-9152-0](https://doi.org/10.1007/s10712-011-9152-0)
- 339 Ban-Weiss, G. A., Cao, L., Bala, G., & Caldeira, K. (2012, March). Dependence of
340 climate forcing and response on the altitude of black carbon aerosols. *Climate*
341 *Dynamics*, *38*(5), 897–911. Retrieved 2020-10-21, from [https://doi.org/10](https://doi.org/10.1007/s00382-011-1052-y)
342 [.1007/s00382-011-1052-y](https://doi.org/10.1007/s00382-011-1052-y) doi: 10.1007/s00382-011-1052-y
- 343 Bellouin, N., Quaas, J., Gryspeerdt, E., Kinne, S., Stier, P., Watson-
344 Parris, D., ... Stevens, B. (2020). Bounding Global Aerosol Ra-

- 345 diative Forcing of Climate Change. *Reviews of Geophysics*, 58(1),
 346 e2019RG000660. Retrieved 2021-02-01, from [https://agupubs](https://agupubs.onlinelibrary.wiley.com/doi/abs/10.1029/2019RG000660)
 347 [.onlinelibrary.wiley.com/doi/abs/10.1029/2019RG000660](https://agupubs.onlinelibrary.wiley.com/doi/abs/10.1029/2019RG000660) (eprint:
 348 <https://agupubs.onlinelibrary.wiley.com/doi/pdf/10.1029/2019RG000660>) doi:
 349 <https://doi.org/10.1029/2019RG000660>
- 350 Ceppi, P., Brient, F., Zelinka, M. D., & Hartmann, D. L. (2017). Cloud feedback
 351 mechanisms and their representation in global climate models. *Wiley Inter-*
 352 *disciplinary Reviews: Climate Change*, 8(4), e465. Retrieved 2019-07-15,
 353 from <https://onlinelibrary.wiley.com/doi/abs/10.1002/wcc.465> doi:
 354 10.1002/wcc.465
- 355 Chung, E.-S., & Soden, B. J. (2015, March). An Assessment of Direct Radiative
 356 Forcing, Radiative Adjustments, and Radiative Feedbacks in Coupled
 357 Ocean–Atmosphere Models. *Journal of Climate*, 28(10), 4152–4170. Retrieved
 358 2019-07-15, from [https://journals.ametsoc.org/doi/full/10.1175/](https://journals.ametsoc.org/doi/full/10.1175/JCLI-D-14-00436.1)
 359 [JCLI-D-14-00436.1](https://journals.ametsoc.org/doi/full/10.1175/JCLI-D-14-00436.1) doi: 10.1175/JCLI-D-14-00436.1
- 360 Colman, R. A., & McAvaney, B. J. (2011, April). On tropospheric adjustment to
 361 forcing and climate feedbacks. *Climate Dynamics*, 36(9), 1649. Retrieved
 362 2019-09-20, from <https://doi.org/10.1007/s00382-011-1067-4> doi:
 363 10.1007/s00382-011-1067-4
- 364 Conley, A. J., Lamarque, J.-F., Vitt, F., Collins, W. D., & Kiehl, J. (2013, April).
 365 PORT, a CESM tool for the diagnosis of radiative forcing. *Geoscientific Model*
 366 *Development*, 6(2), 469–476. Retrieved 2019-07-15, from [https://www.geosci-](https://www.geosci-model-dev.net/6/469/2013/)
 367 [model-dev.net/6/469/2013/](https://www.geosci-model-dev.net/6/469/2013/) doi: <https://doi.org/10.5194/gmd-6-469-2013>
- 368 Dinh, T., & Fueglistaler, S. (2017). Mechanism of Fast Atmospheric Energetic Equi-
 369 libration Following Radiative Forcing by CO₂. *Journal of Advances in Mod-*
 370 *eling Earth Systems*, 9(7), 2468–2482. Retrieved 2019-07-15, from [https://](https://agupubs.onlinelibrary.wiley.com/doi/abs/10.1002/2017MS001116)
 371 agupubs.onlinelibrary.wiley.com/doi/abs/10.1002/2017MS001116 doi:
 372 10.1002/2017MS001116
- 373 Doutriaux-Boucher, M., Webb, M. J., Gregory, J. M., & Boucher, O. (2009). Car-
 374 bon dioxide induced stomatal closure increases radiative forcing via a rapid
 375 reduction in low cloud. *Geophysical Research Letters*, 36(2). Retrieved 2019-
 376 09-20, from [https://agupubs.onlinelibrary.wiley.com/doi/abs/10.1029/](https://agupubs.onlinelibrary.wiley.com/doi/abs/10.1029/2008GL036273)
 377 [2008GL036273](https://agupubs.onlinelibrary.wiley.com/doi/abs/10.1029/2008GL036273) doi: 10.1029/2008GL036273
- 378 Forster, P. M., Richardson, T., Maycock, A. C., Smith, C. J., Samset, B. H., Myhre,
 379 G., ... Schulz, M. (2016). Recommendations for diagnosing effective radiative
 380 forcing from climate models for CMIP6. *Journal of Geophysical Research:*
 381 *Atmospheres*, 121(20), 12,460–12,475. Retrieved 2020-01-21, from [https://](https://agupubs.onlinelibrary.wiley.com/doi/abs/10.1002/2016JD025320)
 382 agupubs.onlinelibrary.wiley.com/doi/abs/10.1002/2016JD025320 doi:
 383 10.1002/2016JD025320
- 384 Gregory, J., & Webb, M. (2008, January). Tropospheric Adjustment Induces
 385 a Cloud Component in CO₂ Forcing. *Journal of Climate*, 21(1), 58–71.
 386 Retrieved 2019-07-15, from [https://journals.ametsoc.org/doi/full/](https://journals.ametsoc.org/doi/full/10.1175/2007JCLI1834.1)
 387 [10.1175/2007JCLI1834.1](https://journals.ametsoc.org/doi/full/10.1175/2007JCLI1834.1) doi: 10.1175/2007JCLI1834.1
- 388 Hansen, J., Sato, M., & Ruedy, R. (1997). Radiative forcing and climate response.
 389 *Journal of Geophysical Research: Atmospheres*, 102(D6), 6831–6864. Retrieved
 390 2019-08-09, from [https://agupubs.onlinelibrary.wiley.com/doi/abs/](https://agupubs.onlinelibrary.wiley.com/doi/abs/10.1029/96JD03436)
 391 [10.1029/96JD03436](https://agupubs.onlinelibrary.wiley.com/doi/abs/10.1029/96JD03436) doi: 10.1029/96JD03436
- 392 Hartmann, D. L. (1994). *Global physical climatology*. San Diego ; London: Academic
 393 Press.
- 394 Kamae, Y., Chadwick, R., Ackerley, D., Ringer, M., & Ogura, T. (2019, May).
 395 Seasonally variant low cloud adjustment over cool oceans. *Climate Dynamics*,
 396 52(9-10), 5801–5817. Retrieved 2019-09-16, from [http://link.springer.com/](http://link.springer.com/10.1007/s00382-018-4478-7)
 397 [10.1007/s00382-018-4478-7](http://link.springer.com/10.1007/s00382-018-4478-7) doi: 10.1007/s00382-018-4478-7
- 398 Kamae, Y., & Watanabe, M. (2012). On the robustness of tropo-
 399 spheric adjustment in CMIP5 models. *Geophysical Research Let-*

- ters, 39(23). Retrieved 2020-04-28, from <https://agupubs.onlinelibrary.wiley.com/doi/abs/10.1029/2012GL054275> (eprint: <https://agupubs.onlinelibrary.wiley.com/doi/pdf/10.1029/2012GL054275>) doi: 10.1029/2012GL054275
- Kamae, Y., & Watanabe, M. (2013, December). Tropospheric adjustment to increasing CO₂: its timescale and the role of land–sea contrast. *Climate Dynamics*, 41(11–12), 3007–3024. Retrieved 2019-07-04, from <http://link.springer.com/10.1007/s00382-012-1555-1> doi: 10.1007/s00382-012-1555-1
- Kamae, Y., Watanabe, M., Ogura, T., Yoshimori, M., & Shiogama, H. (2015, June). Rapid Adjustments of Cloud and Hydrological Cycle to Increasing CO₂: a Review. *Current Climate Change Reports*, 1(2), 103–113. Retrieved 2019-07-04, from <http://link.springer.com/10.1007/s40641-015-0007-5> doi: 10.1007/s40641-015-0007-5
- Klein, S. A., & Hartmann, D. L. (1993, August). The Seasonal Cycle of Low Stratiform Clouds. *Journal of Climate*, 6(8), 1587–1606. Retrieved 2020-12-18, from https://journals.ametsoc.org/view/journals/clim/6/8/1520-0442_1993_006_1587_tscols_2_0_co_2.xml (Publisher: American Meteorological Society Section: Journal of Climate) doi: 10.1175/1520-0442(1993)006<1587:TSCOLS>2.0.CO;2
- Koch, D., & Del Genio, A. D. (2010, August). Black carbon semi-direct effects on cloud cover: review and synthesis. *Atmospheric Chemistry and Physics*, 10(16), 7685–7696. Retrieved 2021-01-25, from <https://acp.copernicus.org/articles/10/7685/2010/> doi: 10.5194/acp-10-7685-2010
- Myhre, G., Forster, P. M., Samset, B. H., Hodnebrog, O., Sillmann, J., Aalbergstjø, S. G., ... Zwiers, F. (2017, June). PDRMIP A Precipitation Driver and Response Model Intercomparison Project—Protocol and Preliminary Results. *Bulletin of the American Meteorological Society*, 98(6), 1185–1198. Retrieved 2019-08-01, from <http://journals.ametsoc.org/doi/10.1175/BAMS-D-16-0019.1> doi: 10.1175/BAMS-D-16-0019.1
- Myhre, G., Shindell, D., Bréon, F.-M., Collins, W., Fuglestedt, J., Huang, J., ... Zhang, H. (2014). *Anthropogenic and Natural Radiative Forcing*. In: *Climate Change 2013: The Physical Science Basis. Contribution of Working Group I to the Fifth Assessment Report of the Intergovernmental Panel on Climate Change* (Tech. Rep. No. AR5). Retrieved from <https://www.ipcc.ch/report/ar5/wg1/> (Publisher: Cambridge University Press)
- Neale, R. B., Richter, J. H., Conley, A. J., Park, S., Lauritzen, P. H., Gettelman, A., ... Lin, S.-J. (2010, April). *Description of the NCAR Community Atmosphere Model (CAM 4.0)*.
- Richardson, T. B., Forster, P. M., Smith, C. J., Maycock, A. C., Wood, T., Andrews, T., ... Watson-Parris, D. (2019). Efficacy of Climate Forcings in PDRMIP Models. *Journal of Geophysical Research: Atmospheres*, 124(23), 12824–12844. Retrieved 2020-01-17, from <https://agupubs.onlinelibrary.wiley.com/doi/abs/10.1029/2019JD030581> doi: 10.1029/2019JD030581
- Samset, B. H., & Myhre, G. (2015). Climate response to externally mixed black carbon as a function of altitude. *Journal of Geophysical Research: Atmospheres*, 120(7), 2913–2927. Retrieved 2019-10-04, from <https://agupubs.onlinelibrary.wiley.com/doi/abs/10.1002/2014JD022849> doi: 10.1002/2014JD022849
- Sherwood, S. C., Bony, S., Boucher, O., Bretherton, C., Forster, P. M., Gregory, J. M., & Stevens, B. (2015, February). Adjustments in the Forcing-Feedback Framework for Understanding Climate Change. *Bulletin of the American Meteorological Society*, 96(2), 217–228. Retrieved 2020-12-10, from <https://journals.ametsoc.org/view/journals/bams/96/2/bams-d-13-00167.1.xml> (Publisher: American Meteorological Society Section: Bulletin of the American

- 455 Meteorological Society) doi: 10.1175/BAMS-D-13-00167.1
- 456 Shine, K., Fouquart, Y., Ramaswamy, V., Solomon, S., & Srinivasan, J. (1995).
 457 *Radiative Forcing. In: IPCC Report on Radiative Forcing of Climate Change*
 458 *and An Evaluation of the IPCC IS92 Emission Scenarios* (Tech. Rep.). Re-
 459 trieved 2021-01-14, from [https://www.ipcc.ch/report/climate-change-](https://www.ipcc.ch/report/climate-change-1994-radiative-forcing-of-climate-change-and-an-evaluation-of-the-ipcc-is92-emission-scenarios-2/)
 460 [-1994-radiative-forcing-of-climate-change-and-an-evaluation-of-the-](https://www.ipcc.ch/report/climate-change-1994-radiative-forcing-of-climate-change-and-an-evaluation-of-the-ipcc-is92-emission-scenarios-2/)
 461 [-ipcc-is92-emission-scenarios-2/](https://www.ipcc.ch/report/climate-change-1994-radiative-forcing-of-climate-change-and-an-evaluation-of-the-ipcc-is92-emission-scenarios-2/)
- 462 Shine, K. P., Cook, J., Highwood, E. J., & Joshi, M. M. (2003). An
 463 alternative to radiative forcing for estimating the relative impor-
 464 tance of climate change mechanisms. *Geophysical Research Let-*
 465 *ters*, 30(20). Retrieved 2021-01-11, from [https://agupubs](https://agupubs.onlinelibrary.wiley.com/doi/abs/10.1029/2003GL018141)
 466 [.onlinelibrary.wiley.com/doi/abs/10.1029/2003GL018141](https://agupubs.onlinelibrary.wiley.com/doi/abs/10.1029/2003GL018141) (eprint:
 467 <https://agupubs.onlinelibrary.wiley.com/doi/pdf/10.1029/2003GL018141>) doi:
 468 <https://doi.org/10.1029/2003GL018141>
- 469 Smith, C. J., Kramer, R. J., Myhre, G., Alterskjær, K., Collins, W., Sima, A.,
 470 ... Forster, P. M. (2020, January). *Effective radiative forcing and ad-*
 471 *justments in CMIP6 models* (preprint). Radiation/Atmospheric Mod-
 472 elling/Troposphere/Physics (physical properties and processes). Re-
 473 trieved 2020-02-05, from [https://www.atmos-chem-phys-discuss.net/](https://www.atmos-chem-phys-discuss.net/acp-2019-1212/)
 474 [acp-2019-1212/](https://www.atmos-chem-phys-discuss.net/acp-2019-1212/) doi: 10.5194/acp-2019-1212
- 475 Smith, C. J., Kramer, R. J., Myhre, G., Forster, P. M., Soden, B. J., Andrews, T.,
 476 ... Watson-Parris, D. (2018). Understanding Rapid Adjustments to Diverse
 477 Forcing Agents. *Geophysical Research Letters*, 45(21), 12,023–12,031. Re-
 478 trieved 2019-07-15, from [https://agupubs.onlinelibrary.wiley.com/doi/](https://agupubs.onlinelibrary.wiley.com/doi/abs/10.1029/2018GL079826)
 479 [abs/10.1029/2018GL079826](https://agupubs.onlinelibrary.wiley.com/doi/abs/10.1029/2018GL079826) doi: 10.1029/2018GL079826
- 480 Stjern, C. W., Samset, B. H., Boucher, O., Iversen, T., Lamarque, J.-F., Myhre,
 481 G., ... Takemura, T. (2020, November). How aerosols and greenhouse
 482 gases influence the diurnal temperature range. *Atmospheric Chemistry*
 483 *and Physics*, 20(21), 13467–13480. Retrieved 2021-02-01, from [https://](https://acp.copernicus.org/articles/20/13467/2020/)
 484 acp.copernicus.org/articles/20/13467/2020/ (Publisher: Copernicus
 485 GmbH) doi: <https://doi.org/10.5194/acp-20-13467-2020>
- 486 Swales, D. J., Pincus, R., & Bodas-Salcedo, A. (2018, January). The Cloud Feed-
 487 back Model Intercomparison Project Observational Simulator Package: Version
 488 2. *Geoscientific Model Development*, 11(1), 77–81. Retrieved 2021-01-12,
 489 from <https://gmd.copernicus.org/articles/11/77/2018/> (Publisher:
 490 Copernicus GmbH) doi: <https://doi.org/10.5194/gmd-11-77-2018>
- 491 Zelinka, M. D., Klein, S. A., & Hartmann, D. L. (2012, June). Computing and
 492 Partitioning Cloud Feedbacks Using Cloud Property Histograms. Part II:
 493 Attribution to Changes in Cloud Amount, Altitude, and Optical Depth. *Jour-*
 494 *nal of Climate*, 25(11), 3736–3754. Retrieved 2020-04-28, from [https://](https://journals.ametsoc.org/doi/full/10.1175/JCLI-D-11-00249.1)
 495 journals.ametsoc.org/doi/full/10.1175/JCLI-D-11-00249.1 (Publisher:
 496 American Meteorological Society) doi: 10.1175/JCLI-D-11-00249.1
- 497 Zelinka, M. D., Klein, S. A., Taylor, K. E., Andrews, T., Webb, M. J., Gre-
 498 gory, J. M., & Forster, P. M. (2013, January). Contributions of Differ-
 499 ent Cloud Types to Feedbacks and Rapid Adjustments in CMIP5. *Jour-*
 500 *nal of Climate*, 26(14), 5007–5027. Retrieved 2019-07-15, from [https://](https://journals.ametsoc.org/doi/full/10.1175/JCLI-D-12-00555.1)
 501 journals.ametsoc.org/doi/full/10.1175/JCLI-D-12-00555.1 doi:
 502 10.1175/JCLI-D-12-00555.1